A&A 486, 331–340 (2008)
DOI: 10.1051/0004-6361:20077454

Astronomy & Astrophysics

Evolution of the crystallization front in cometary models

Effect of the net energy released during crystallization

M. González, P. J. Gutiérrez, L. M. Lara, and R. Rodrigo

Instituto de Astrofísica de Andalucía-CSIC, PO Box 3004, 18080 Granada, Spain
e-mail: marta@iaa.es

Received 12 March 2007 / Accepted 9 April 2008

ABSTRACT

Context. It is plausible that at least part of the water ice of cometary nuclei is initially in an amorphous phase, doped with other volatiles. As the nuclei are heated, the amorphous ice would then transform irreversibly into cubic ice. The net energy liberated in this transformation may be affected by the presence of any impurities because part of the energy liberated during crystallization may be expended in the desorption of dopant elements.

Aims. Our goal is to study the evolution of the crystallization front of the amorphous ice in a simulated nucleus, providing quantitative results. In particular, the influence of the net energy released during crystallization on the thermophysical evolution will be analyzed.

Methods. We use a simplified thermophysical model to simulate a cometary nucleus, where the ice is assumed initially to be in an amorphous phase. The model allows us to estimate the instantaneous rate of crystallization and the time spent in crystallization, for a fixed volume of amorphous ice, as a function of the net energy released. Simulations are performed for different characterizations of the nucleus interior such as dust-to-ice ratio, density, or thermal inertia.

Results. As expected, the evolution of the crystallization front depends strongly on the characteristics of the nucleus interior. If the nucleus interior has, however, a dust-to-ice ratio smaller than 1, and a low thermal inertia, approximately of 20 W K^{-1} m^{-2} $s^{1/2}$, the crystallization front evolves discontinuously, with quasi-periodic increases in the crystallization rate. Those increases have a period that ranges from 1 to 40 days, if the energy released by crystallization is unaffected by impurities. These surges of crystallization could be responsible for the periodic outbursts observed for comet 9P/Tempel 1 shortly before the Deep Impact experiment. The evolution of the crystallization front becomes continuous and almost steady, if the net energy released is half that of the pure, exothermic case, regardless of the characteristics of the nucleus interior. On the other hand, if the dust-to-ice ratio is high (larger than 1) and/or the thermal inertia is high (larger than 100), the crystallization front evolves in a continuous and smooth manner, even for pure, exothermic crystallization.

Other quantitative results, including a comparison with plausible erosion rates, are described.

Key words. comets: general – methods: numerical – solar system: general

1. Introduction

Comets have porous bodies, which are composed of ices and dust, and are a few kilometers in size. Water ice is their principal, volatile constituent, although other volatile compounds, such as CO, CO_2, CH_4, or NH_3, are also present. Comets become highly active, ejecting a significant amount of gas and dust produced by ice sublimation, with solar heating, usually at less than 4 AU from the Sun, although some show activity at larger heliocentric distances (e.g. Hale-Bopp, 29P/Schwassmann-Wachmann 1). Conventionally, bursts of activity interrupt more regular behavior (see e.g. A'Hearn et al. 2005, for comet 9P/Tempel 1). There is no definitive explanation for these outbursts, although various possibilities have been suggested, such as crystallization, surface fragmentation due to the formation of gas pockets, meteoritic impacts, polymerization of hydrogen cyanide, HCN, and destruction of cometary grains under strong solar wind (see for example the review of the different sources for the outbursts by Gronkowski 2007, and references therein). Activity is presently poorly understood, mainly because our knowledge of the internal structure of cometary nuclei, its formation, and evolution, is scarce. There is, for example, no direct and simple correspondence between heliocentric distance and the volatility of the constituents (see e.g. Capria 2002). This suggests that highly volatile constituents, or at least part of them, may be trapped within the water-ice structure. Nevertheless, the processes involved in their trapping, and storing, and therefore the internal distribution of this dust-ice mixture is unknown or, at least, controversial. There is evidence that cometary nuclei formed at low temperature and pressure. Thus, one possible explanation is that water ice condensed in the amorphous phase, when it was able to trap other volatile compounds within its structure. This idea could be supported with observations of icy grains in the coma of some comets, such as C/2002 C7 and Hale-Bopp. Near-infrared spectra of the detected icy grains do not show the characteristic 1.65 μm-absorption feature of crystalline ice, which implies that the water ice could be in the amorphous phase (e.g. Davies et al. 1997; Kawakita et al. 2004). Since the spectral feature depends strongly on the temperature, the non-detection of the absorption feature cannot be considered definitive proof of amorphous ice.

Another possibility for gas trapping is the formation of clathrate hydrates. Originally proposed by Delsemme and Swings (1952), the presence of clathrates was included in cometary, thermophysical modeling (e.g. Flammer et al. 1998). Cometary clathrate formation is indeed becoming an attractive explanation, following the Hale-Bopp visit and the analysis of Stardust samples (e.g. Brownlee et al. 2006; Ciesla 2007), which may be consistent with circulation in the solar nebula. Observations exist that could be explained by the presence of

clathrate hydrates, in particular because laboratory experiments point out the difficulty of amorphous ice formation, even for low temperatures (e.g. Moore et al. 1994). These structures consist of a guest molecule surrounded by several molecules of water, which form a cage. The formation of clathrates could explain the under-abundance of N_2 in comets Hale-Bopp, DeVico, and Ikeya-Zhang, and the large variability of CO observed in comets (see e.g. Gautier & Hersant 2005). This is because the order of clathration of the most abundant cometary species, is CH_4, CO and N_2. Since the amount of water molecules is limited, some CO and N_2 molecules may not form clathrates, and they would not be incorporated into, at least, some cometary nuclei. It is necessary to note that the aforementioned under-abundance of certain species can also be explained with amorphous water ice, which is more efficient at trapping CO than N_2 (see e.g. Ehrenfreud et al. 2002, and references therein).

Both proposed mechanisms have arguments for and against, and given our present knowledge (see e.g. Capria 2002; Colangeli et al. 2004), it is difficult to argue definitely in favor of either one of them. Probably, both mechanisms are effective inside cometary nuclei.

We assume that cometary nuclei are formed initially from amorphous ice, and that consequently highly-volatile constituents are trapped. We explore some of the consequences of this assumption. We study the evolution of the crystallization front, with a high, temporal resolution, and in particular, the role of volatile desorption on the energy budget of a body composed of impure amorphous water-ice. Our goal is to quantify how the net energy released during crystallization can affect the cometary, thermophysical evolution, and the physical circumstances under which the effects would be most significant.

2. Antecedents and motivation

Amorphous solid water is a metastable form of ice: it crystallizes into cubic ice, according to an activation law that depends on temperature. For pure, water ice, crystallization is exothermic, with a release of energy that ranges from 5×10^4 to 10^5 J kg^{-1}, see Table 2 in Hallbrucker & Mayer (1987) for a summary, although the usual value assumed in cometary models is that of Ghormley (1968), i.e. 9×10^4 J kg^{-1}. The situation may differ for impure amorphous water ice. As described before, the open structure of amorphous water ice can trap volatiles that would be liberated during the phase change (see e.g. Bar-Nun et al. 1985; Bar-Nun & Laufer 2003; Collings et al. 2003). Their energetic contribution, however, is not yet clear.

In a cometary context, several models have dealt with crystallization (e.g. Klinger 1981; Herman & Podolak 1985; Espinasse et al. 1991, etc.). Most cometary models describe the net energy released by crystallization in a similar way (see, e.g. Prialnik 1992). This energy is calculated to be that of pure amorphous water ice, minus the desorption energy of the dopant, and weighted by the fraction of trapped volatile inside the matrix. Some models (e.g. Prialnik 1992; Tancredi et al. 1994) consider crystallization to be an almost purely exothermic process. In these cases, the energy absorbed to liberate the dopants from the amorphous matrix, is calculated to be $u^{\rm gas} - u^{\rm am}$, where $u^{\rm gas}$ and $u^{\rm am}$ are the specific, internal energies of the (dopant) gas and amorphous ice, respectively. For CO, (the second, most-abundant, volatile component in cometary nuclei, as inferred by observations), these authors estimate $u^{\rm gas}$ to be, approximately, 6×10^4 J kg^{-1} of trapped gas. This value provides a small contribution to the net energy released, since the fraction of gas trapped in the amorphous matrix is small (for comets, usually less than 10% of water ice, in mass). In these cases, crystallization constitutes an important internal-source of energy, evolving as a runaway process. This is why crystallization was proposed to be a possible cause of outbursts observed in comets.

Laboratory experiments indicate, however, that the energy absorbed by desorption of volatile dopants, trapped in the amorphous water ice, could be far higher than the above-mentioned value. Sandford & Allamandola (1990) calculated the surface, binding energy of CO in H_2O, to be 5.17×10^5 J kg^{-1}, and the volume binding energy to be 1.65×10^6 J kg^{-1} (1.72×10^6 J kg^{-1} for annealed samples), from experimental studies of the sticking efficiencies of deposited gas mixtures. Using both experimental and theoretical results, Manca et al. (2001) and Allouche et al. (1998), estimated that the desorption energy of CO from the surface of water ice was 3.57×10^5 J kg^{-1}. Allouche et al. (1998), from quantum calculations, estimated that the volume, binding energy was four times larger than the surface, binding energy. If the amount of impurities is sufficiently large, the energetic contribution of trapped CO, for the values calculated above, would be similar to the energy produced by the crystallization of pure amorphous water ice. Under these circumstances, crystallization could be endothermic. For non-annealed samples, Sandford & Allamandola (1990) indeed calculated a volume, binding energy that implies crystallization could be endothermic, for quantities of CO larger than 5.5% by mass (with respect to water ice), which is an acceptable percentage for comets. These results are in line with those of Kouchi & Sirono (2001), which were derived for experiments of Differential Thermal Analysis (DTA), on amorphous samples doped with various volatiles. These authors found that crystallization was endothermic, when CO impurities were larger than 3% by mass.

Few cometary models have assumed that crystallization can be endothermic. Of those that have, Sirono & Yamamoto (1999) estimate the energetic contribution of dopants to be equal to the latent heat of sublimation (for CO 2.93×10^5 J kg^{-1}). Enzian et al. (1997) adopted a similar parametrization of the net energy released, although, in their simulations, the quantity of dopant does not exceed the endothermic threshold.

Apart from crystallization, amorphous water ice can affect our system in other ways. The behavior of amorphous water ice, when annealed, is not yet well established. It is agreed that there are two forms of amorphous ice, High and Low Density Amorphous (HDA and LDA, respectively), and that HDA transforms into LDA, and then LDA into cubic ice as temperature increases. A number of Temperature-Programmed Desorption (TPD) experiments that studied the release of trapped volatiles, during annealing of doped amorphous solid water, showed that impurities were liberated at various temperatures, remaining even until the water ice started to sublimate (e.g. Collings et al. 2003; Gálvez et al. 2007, etc.). Jenniskens & Blake (1994) suggested that there is a glass transition before crystallization and that a new relaxed form of amorphous ice coexists in a metastable state with the cubic ice: this would explain why the volatiles are preserved until water sublimation. Other authors believe that this glass transition, if it exists, occurs at temperatures higher than crystallization, and cannot be detected (e.g. Macfarlane & Angell 1984; or Yue & Angell 2004). The influence of impurities on the behavior of these ices goes beyond altering only the energy released by crystallization, as the volatile species can experience other energetically-significant processes, such as flux through the ice matrix or recondensation.

We are interested mostly in the evolution of the crystallization front, and the effect of the energy liberated by crystallization, when part of it is absorbed in the desorption of

occluded gases. Due to the lack of agreement in measurements of the different energies involved, we evaluate the impact of the net-energy release, during the crystallization process, on the evolution rate of the crystallization front, and therefore on the cometary, thermophysical evolution.

In the following sections, we describe the model used in our investigations, the results obtained, and our conclusions.

3. Model

The equations that describe the thermophysical evolution of our simulated, cometary nucleus are the mass- and energy- conservation laws. We consider the single spatial component to be the radial one, z. Lateral heat-conduction is neglected because of the low conductivity of cometary material (see e.g. Prialnik et al. 2004). Our nucleus is a porous, solid matrix, made of amorphous water ice and dust, with water vapor filling its pores. The dust is the non-volatile refractory material, and is considered to be a static component in our model.

Thus, the equations to be solved are:

$$\frac{\partial \rho^{\rm am}}{\partial t} = -\lambda \rho^{\rm am} \tag{1}$$

$$\frac{\partial \rho^{\rm cr}}{\partial t} = \lambda \rho^{\rm am} - \frac{\partial \rho^{\rm vap}}{\partial t} - \nabla \cdot J_{\rm H_2O} \tag{2}$$

$$\rho^{\rm vap} = \rho^{\rm sat}(T) \tag{3}$$

$$\sum_{\alpha} \rho^{\alpha} c^{\alpha} \frac{\partial T}{\partial t} = \nabla \cdot (K \nabla T) - H_{\rm net} \frac{\partial \rho^{\rm am}}{\partial t} - c^{\rm vap} J_{\rm H_2O} \cdot \nabla T - H_{\rm H_2O} \left(\frac{\partial \rho^{\rm vap}}{\partial t} + \nabla \cdot J_{\rm H_2O} \right) \tag{4}$$

where $\rho^{\rm am}$, $\rho^{\rm cr}$, and $\rho^{\rm vap}$ represent the densities of amorphous ice, cubic ice, and water vapor, respectively; T is the temperature; $\rho^{\rm sat}$ is the saturation density of water vapor, and $H_{\rm H_2O}$ and $H_{\rm net}$ are the latent heat of water sublimation and the net, crystallization energy, respectively, where the latter is the parameter modified in our calculations. We note that $H_{\rm net}$ includes the contribution of the dopants trapped in the amorphous matrix. The parameter c^{α} represents the specific heat of each species, and $J_{\rm H_2O}$ is the water flow through pores, which is assumed to be described by the Knudsen regime (see, e.g. Prialnik 1992). We assume that water vapor filling the pores, is in equilibrium with ice, allowing only the sublimation required to maintain this equilibrium and the subsequent gas flux (see Tancredi et al. 1994). In any case, gas flux and sublimation are energetically negligible under our conditions. The final two terms in Eqs. (2) and (4) are therefore included only for consistency. In Eq. (4), K is the conductivity of the ice matrix, which is parametrized by:

$$K = (1-p)^{\frac{2}{3}} h \frac{K_{\rm am}\rho^{\rm am} + K_{\rm cr}\rho^{\rm cr} + K_{\rm dust}\rho^{\rm dust}}{\rho^{\rm am} + \rho^{\rm cr} + \rho^{\rm dust}} \tag{5}$$

where K_{α} and ρ^{α} are the conductivity and density of each solid component α, h represents the Hertz factor, which is a correction included to account for the area of contact between individual grains, and the first multiplicative factor is a correction for the porosity $p = 1 - \frac{\rho^{\rm am}+\rho^{\rm cr}}{\rho^{\rm H_2O,c}} - \frac{\rho^{\rm dust}}{\rho^{\rm dust,c}}$, where $\rho^{\alpha,c}$ represents the compact density of each solid. In our simulations, the value of porosity is altered as the component densities change.

The activation law for crystallization, λ, is given by (Schmitt et al. 1989):

$$\lambda(T) = 1.05 \times 10^{13} {\rm e}^{-\frac{5370}{T}}. \tag{6}$$

Crystallization and heat conduction through the ice matrix, are considered to be the two dominant, energetic processes in our simulations, since we are evaluating the effect of a single variable, which is the net energy released in the crystallization of amorphous ice. Calculations are performed for a simulated nucleus with a fixed surface temperature, and simulations, for temperatures of 140, 150, and 160 K. In principle, a constant temperature could be a first approximation of the temperature in the nucleus interior, several skin-depths below the surface and therefore not significantly affected by rotational variability. The upper limit to the temperature, 160 K, was chosen because it is sufficiently low to avoid significant, water sublimation. In the worst-case simulations, for which the highest energy was released, the energetic contribution of sublimation at the surface is below 2.5% of the heat conducted into the interior. We could use a different boundary condition at the surface, such as the energy balance between the solar flux received, the energy re-radiated, and the energy spent in sublimation and the gas flux (see e.g. Tancredi et al. 1994). The problem is that in that case water sublimation would not be negligible, because the surface temperature would probably exceed 170 K, at least for the highest values of released energy.

Inside the interior of the nucleus, our boundary conditions are null heat and vapor fluxes, which are valid only when applied at sufficiently large depth. We note that from a numerical standpoint, equations are discretized with finite differences, using a Crank-Nicolson approximation scheme.

We note that, when assuming that impurities modify the energy released during crystallization, we implicitly assume that desorption occurs at similar temperatures as crystallization. If we assume that desorption happens at lower temperatures, the energy released on the phase transition, would be similar to that of pure water ice, but the energy of desorption would be consumed before crystallization.

3.1. Model parameters

From a thermophysical point-of-view, there are other variables, besides the net energy released during crystallization, whose values, for comets, are not known accurately, but are critical for cometary-nucleus modeling. In particular, it is expected that the evolution of the crystallization front is very sensitive to the internal temperature. A typical value of the initial, internal temperature in cometary modeling is 30 K. In principle, such a low internal temperature, which could find support from, for example, the detection of S_2, a highly volatile molecule that requires a low temperature to remain in a condensed phase, may have a strong influence on the crystallization-front evolution-rate. This is because a significant time is taken to raise the temperature to the level at which crystallization starts. In our simulations, initial, internal temperatures of both 30 K and 70 K, the latter of which, was arbitrarily chosen, were assumed. The effects of the initial, temperature profile are discussed in the results section. An initial temperature higher than 70 K, such as approximately 100 K, would produce, almost simultaneously, a crystallization of the entire volume. It would then become difficult to define the crystallization front and measure its evolution rate.

In cometary models, other quantities that affect the crystallization-front evolution but are not accurately defined, are the amorphous ice content, which is directly related to the energy released inside the nucleus, and the thermal inertia, which is directly related to the rate at which heat diffuses into the nucleus. Both of these quantities are in turn dependent on variables such as porosity, density, and dust-to-ice ratio, which are also

poorly constrained. Although there is agreement that comets are fluffy conglomerates, for which porosities higher than 0.65 are usually invoked, (see e.g. Davidsson et al. 2007, and references therein), no accurate measurements of porosity exist. In our simulations, porosities ranging from 0.3 up to 0.8 were considered. Measurements of the dust-to-ice ratio were calculated from observations; these ratios are poorly constrained, and estimated for the coma, which may not be representative of the dust-to-ice ratio in the nucleus. Measurements for the Deep Impact experiment imply that the ratios are large, ranging from 1 to 100, depending on the mass exponent and cut-off mass used (see e.g. Küppers et al. 2005). These estimates could reflect the stratigraphy of the nucleus, which could have an outer dusty layer and an ice-rich interior (Sunshine et al. 2007). This implies that the actual dust-to-ice ratio may be between a value smaller than 1 and values much larger than 1. In our simulations, a dust-to-ice ratio ranging from 0.1 up to 20 is considered. The two variables mentioned above are related to the comet bulk density, which is also poorly constrained. Although measurements (e.g. Davidsson & Gutiérrez 2004, 2005, 2006), including that of Tempel 1 from the DI experiment (Richardson & Melosh 2006) are consistent with a mean value of about 400–500 kg m^{-3}, the uncertainty error bar is large, of about 300 kg m^{-3}. Our simulations cover densities that range from 250 up to 700 kg m^{-3}. Measurements of thermal inertia, which is related to previous variables, for Tempel 1, are consistent with values below 50 W K^{-1} m^{-2} s$^{1/2}$ (Lisse et al. 2005; Groussin et al. 2007). Thermal-inertia measurements derived from thermal emission, as for the measurements presented above, are, however, model dependent. This was pointed out by Davidsson et al. (2007), who showed that two different thermophysical models require different thermal inertias, ranging from 100 up to 400 W K^{-1} m^{-2} s$^{1/2}$, to reproduce identical non-gravitational changes in the orbit. In light of the surface-composition measurements of Sunshine et al. (2007), the low value of 50 W K^{-1} m^{-2} s$^{1/2}$ could correspond to the thermal inertia of the refractory material alone. In our simulations, we consider a thermal inertia, controlled mainly by the dust-to-ice ratio and the Hertz factor, that ranges from 20 up to 400 W K^{-1} m^{-2} s$^{1/2}$ [1].

Given the uncertainty in all of the aforementioned variables, the simulations cover a range of plausible values for them, as summarized in Table 1. It is necessary to keep in mind that some of them are coupled (e.g. porosity, dust-to-ice ratio, bulk density, thermal inertia, etc.). In this respect, the change of a variable leads, generally, to a change in the others, and not all variable combinations reflect physically meaningful values, according to our present knowledge of comets. In all simulations performed, all parameters were retained within specified limits. In Table 1, parameter values for pure substances are in-between the values in the cometary models, which are taken from Tancredi et al. (1994), Prialnik et al. (2004) and Enzian et al. (1997).

4. Results and discussion

All of the following results are described for a surface temperature of 160 K. At the end of the section, the effect of this boundary condition is discussed.

[1] The values for the thermal inertia were estimated for a temperature of 140 K, assuming that the ice is in the crystalline phase.

Table 1. Values of the parameters used in the simulations. The effect of some variables on the results was studied by altering their values within a plausible range. For example, several values of porosities, dust-to-ice ratios, and thermal inertia were used in the simulations.

Parameter	Value(s)	Units
Surface temperature	140, 150, 160	K
R_g	8.314	J K^{-1} mol^{-1}
μ	18.	g mol^{-1}
$\rho^{H_2O,c}$	920.	kg m^{-3}
$\rho^{dust,c}$	2500.	kg m^{-3}
c^{H_2O}	7.49·T+90.	J kg^{-1} K^{-1}
c^{dust}	5.·T	J kg^{-1}K^{-1}
K_{am}	$7.1 \times 10^{-5}T$	W m^{-1}K^{-1}
K_{cr}	567./T	W m^{-1}K^{-1}
K_{dust}	2.	W m^{-1}K^{-1}
T (initial)	30., 70	K
ρ^{am}(initial)	19–636	kg m^{-3}
ρ^{dust}	36–667	kg m^{-3}
p (initial porosity)	0.28–0.82	
bulk density	250, 400, 700	kg m^{-3}
Thermal inertia	20, 100, 400	W K^{-1} m^{-2} s$^{1/2}$
dust-to-ice ratio	0.1, 1, 20	
radius	1000	m
depth	5	m

4.1. Local rate of crystallization

We study the local or instantaneous rate of crystallization, r_c, and the effect of the net energy released. This local rate is defined to be

$$r_c = \frac{|\Delta\rho^{am}|}{\Delta t}, \quad (7)$$

which estimates the amount of amorphous ice that is crystallized at each time step, providing us with a general view of the process development. As an example, Fig. 1 shows the local rate versus time for three net energies released during crystallization: first, the pure exothermic case (panel (a)); second, a simulation in which it is assumed that half of the energy liberated in crystallization is absorbed by the desorption of dopants (that is $H_{net} = 4.5\times10^4$ J kg^{-1}, panel (b)); and third, the result of a model in which the crystallization is neutral from an energetic point-of-view (panel (c)). In addition, these simulations were performed for a density of 400 kg m^{-3}, a dust-to-ice ratio of 1.0, a thermal inertia of 20 W K^{-1} m^{-2} s$^{1/2}$, and an initial, internal temperature of 70 K. This parameter set, which can be considered to be the nominal case, allows us to illustrate the different behaviors shown by r_c in our simulations.

From Fig. 1, both the quantitative and qualitative dependence of crystallization rate on the net energy released, is clearly evident. When the net energy released by crystallization is that of pure amorphous water ice (panel (a) in Fig. 1), the rate of crystallization may evolve discontinuously, with repetitive strong "surges", which are, logically, accompanied by respective increases in temperature. If those surges are analyzed in detail, it could be seen that the crystallization evolves comparatively slowly until its rate reaches a value of about 10^5 kg m^{-3} h^{-1}. Then, it increases above 10^6 kg m^{-3} h^{-1} very rapidly. Those surges are quasi-periodic, with the period slightly increasing as the crystallization front evolves toward the interior. This is expected in this kind of static model, in which the energy coming from the upper boundary generally diminishes with depth. In the simulation shown in panel (a) of Fig. 1, spurts show a period of 5–7 days.

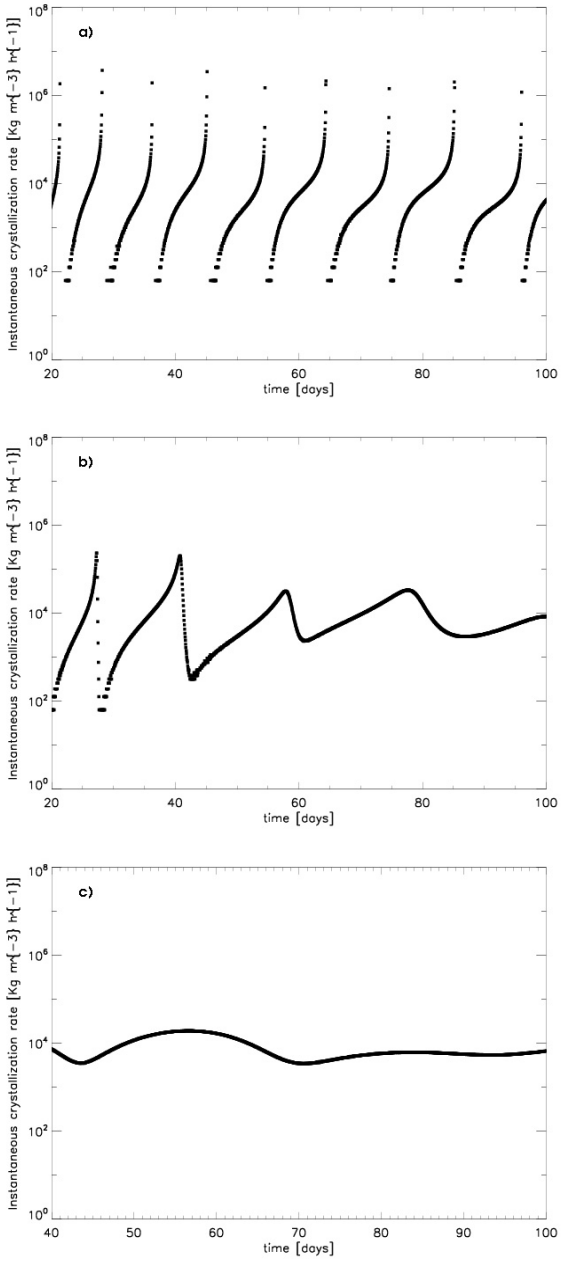

Fig. 1. Local rate of crystallization (kg m^{-3} h^{-1}) against time for simulated nuclei with different net energies released. In this figure, panel **a)** corresponds to a net energy released of $H_{\rm net} = 9 \times 10^4$ J kg^{-1} (that is the maximum energy released by pure amorphous ice, according to standard modelling) in a nucleus with a density of 400 kg m^{-3}, a thermal inertia of 20 W K^{-1} m^{-2} s$^{1/2}$, and a dust-to-ice ratio of 1.0. Panel **b)** corresponds to the same simulated nucleus but setting the net energy released in crystallization as $H_{\rm net} = 4.50 \times 10^4$ J kg^{-1} (half that of pure amorphous ice). Panel **c)** shows the crystallization rate of the same simulated nucleus but in this case, all the energy released during crystallization is spent in desorption of dopant constituents (that is $H_{\rm net} = 0$ J kg^{-1}). In all the simulations the initial temperature is 70 K. These parameters have been chosen to show all the different behaviors of $r_{\rm c}$ appearing in our simulations.

In Fig. 1, it can been seen that the surges of crystallization appear only when the net energy released is high. For the set of parameters corresponding to the simulations shown in Fig. 1, local rate surges do not appear, or appear only at the beginning of the nucleus crystallization, for energies smaller than 50% of the energy liberated for pure amorphous water ice, i.e. smaller than 4.5×10^4 J kg^{-1}. Below that threshold, the energy released is insufficiently high to create the rate spurts. In those cases, the local rate of crystallization evolves in a continuous way. This behavior is illustrated, for example, in panels (b) and (c) of Fig. 1. In panel (b), corresponding to an energy of 4.5×10^4 J kg^{-1}, it can be seen that some peaks appear only at the beginning of the simulation. These initial peaks could be an "edge" effect due to the ΔT height at the start of the calculations, disappearing when the temperature profile becomes smooth. In addition, with the simplified model used in these simulations, it is not possible to say if those initial peaks would propagate into the nucleus if erosion of the surface were taken into account. This would depend, of course, on the balance between the erosion rate and the evolution of the crystallization front, a circumstance which will be discussed in the next section.

The surges in the crystallization rate can be easily explained. When the surface temperature is sufficiently high, crystallization begins, releasing a large amount of energy that produces an increase in the temperature and, consequently, the rate of crystallization. These increased values are maintained until all the amorphous ice in the crystallization front becomes crystalline. At this moment, the energy released diffuses mainly toward the surface, as the conductivity of amorphous ice is extremely low. This circumstance slows down the crystallization. Additional simulations, artificially increasing the thermal conductivity of amorphous ice, show that, if thermal conductivity of the amorphous region is similar to that of the crystalline, spurts of crystallization would not appear.

In general, the apparition of surges in the instantaneous crystallization rate, their separation in time, and the threshold of the net energy released below which the spurts disappear, depend on the balance between the timescales of heat diffusion and crystallization for the local temperature, in the region of the crystallization front. Generally, rate surges appear when the timescale of heat diffusion is longer than that of crystallization. That is, the heat liberated in the crystallization does not diffuse fast enough, and it is accumulated into the volume element, increasing its temperature and, therefore, increasing the crystallization rate. In this problem, the fact that the thermal inertia of amorphous ice is small (several orders of magnitude smaller than that of dust and that of crystalline ice) plays, as mentioned above, a relevant role. Crystallization timescale is the inverse of Eq. (6), which depends on the temperature (and therefore on the net energy released, and on the amorphous ice content). As for the timescale of heat diffusion, it depends on the density, effective heat capacity, effective thermal conductivity, and therefore on the temperature, and on all the densities of the different compounds forming the nucleus (and therefore on the dust-to-ice ratio). We refer the author to Prialnik et al. (2004) for an in-depth description of the different timescales of processes involved in the thermophysical description of a cometary nucleus, including those of crystallization and heat diffusion. Given the strong coupling among the different variables involved in cometary-nucleus modeling, it is not possible to definitively state the effect of a particular variable, without considering the effect of the others. In general, the only secure comment to be made is that every variable that increases the timescale of heat diffusion will increase the period of crystallization surges. Equally, every variable that produces a net decrease in the timescale of heat diffusion, compared to that of crystallization, produces an increase in the frequency of the crystallization spurts or, eventually, a high but smooth crystallization rate. In a similar way, if the energy released is comparatively small (for example, when the ice content is small compared to the dust,

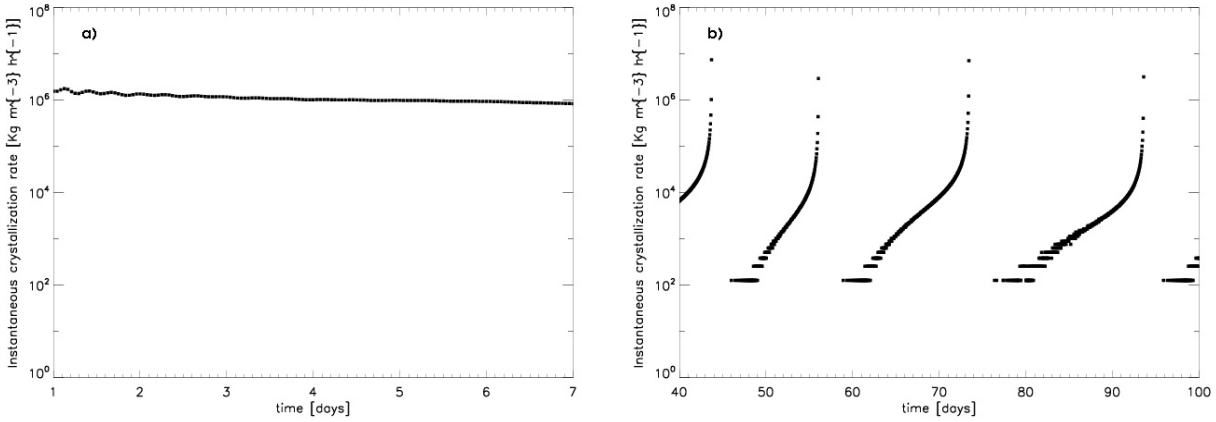

Fig. 2. Panel **a)**: instantaneous crystallization rate for a nucleus with the same characteristics as that of panel **a)** of Fig. 1 except for the thermal inertia. In this case, the thermal inertia is 400 W K^{-1} m^{-2} $s^{1/2}$. Panel **b)**: instantaneous crystallization rate for a nucleus with the same characteristics as in panel **a)** of Fig. 1 except for the density, which is now 700 kg m^{-3}.

or when the dopant components require a significant fraction of energy to be desorbed), the crystallization timescale is similar to or shorter than the timescale of heat diffusion and surges do not appear. In those cases, the crystallization front evolves with a smooth and small rate.

In any case, the simulations performed, allowed us to illustrate the effect of some bulk variables, such as density and thermal inertia. Considering the expressions given in Prialnik et al. (2004), the timescale of heat diffusion can be re-written as

$$\tau_{\rm dif} \propto \frac{\rho^2 C^2}{I} \tag{8}$$

where ρ is the bulk density; C, in this case, is the effective, heat capacity of the material in the crystallization front; and I is the thermal inertia in the crystallization front. With this expression, the effect of the main variables can be clearly seen. For example, both an increase in the thermal inertia and a reduction in the density would imply a reduction in the timescale of heat diffusion. Thus, for example, an increase in the thermal inertia would eventually create the disappearance of the crystallization surges. An increase in the density would also produce an increase in the period of the crystallization spurts. These circumstances can be seen in Fig. 2. Panel (a) of that figure, which shows the crystallization rate of a simulated nucleus that is similar to that of panel (a) of Fig. 1, but now with a thermal inertia of 400 W K^{-1} m^{-2} $s^{1/2}$. It can be seen that after increasing the thermal inertia, and consequently, diminishing the timescale of heat diffusion, crystallization surges do not appear, even if the net energy released is that of amorphous pure ice. For the density, dust-to-ice ratio, and the other parameters corresponding to those simulations, crystallization spurts do not appear, even for a thermal inertia of 100 W K^{-1} m^{-2} $s^{1/2}$. To achieve crystallization surges for a thermal inertia of 100 W K^{-1} m^{-2} $s^{1/2}$, it is necessary to decrease the dust-to-ice ratio, and therefore increase the net energy released within the crystallization front, and diminish the density, to reduce the timescale of heat diffusion. For example, for a dust-to-ice ratio of 0.1, a density of 250 kg m^{-3}, and a thermal inertia of 100 W K^{-1} m^{-2} $s^{1/2}$, crystallization surges appear approximately every day.

Panel (b) of Fig. 2 shows the inverse behavior. This simulation corresponds to the same simulated nucleus as in panel (a) of Fig. 1, but in this case, the bulk density is 700 kg m^{-3}. It can be seen that the increase in density translates into an increase in the period of the crystallization surges, now appearing every 15–20 days.

Other magnitudes, such as the dust-to-ice ratio, directly related to the total, net energy released, and the internal temperature also have an important impact. Logically, the larger the dust-to-ice ratio, and the higher the internal temperature, the longer is the period of the crystallization spurts. Eventually, a large dust-to-ice ratio may lead to the disappearance of the surges. In our simulations, nuclei with a dust-to-ice ratio of 20 do not show any spurt in the crystallization rate, even when the net energy released is that of pure amorphous ice. This is not only due to the fact that there is less ice, but also to the fact that the thermal conductivity is controlled mostly by the dust, allowing substantial heat diffusion into the interior. Additional simulations in which the dust-to-ice ratio is varied, and the remainder parameters are maintained within the ranges given in Table 1, show that surges in the rate of crystallization disappear for dust-to-ice ratios larger than approximately 5.

In summary, the net energy released in crystallization significantly affects the evolution of the local rate of crystallization. The crystallization may evolve in a discontinuous manner, with strong and repetitive increases in its rate, if the energy released during crystallization is comparatively high. Considering the entire set of simulations, surges of crystallization may appear with a period ranging from the order of 1 day (when the dust-to-ice ratio is ∼0.1, the density is low ∼250 kg m^{-3}, and the thermal inertia is moderate ∼100 W K^{-1} m^{-2} $s^{1/2}$), up to the order of 1 month (when the density is ∼700 kg m^{-3}, and the thermal inertia is small, ∼20 W K^{-1} m^{-2} $s^{1/2}$). From our simulations, and regardless of the physical characteristics of the nucleus (within the range given in Table 1), crystallization surges do not appear when the net energy released is smaller than 4.5×10^4 J kg^{-1}, that is half the energy released in the crystallization of pure, amorphous ice. For the energy reported by Sandford & Allamandola (1990) for the volume, binding energy in non-annealed samples, this would imply that a 2.73% (in mass) of impurities would be sufficient to produce a smooth evolution of the crystallization front.

This last statement requires additional consideration. On the one hand, it is necessary to bear in mind that this energy threshold may increase for particular physical characteristics of the nucleus. For example, for a comparatively-high, thermal inertia (above 100 W K^{-1} m^{-2} $s^{1/2}$) and/or a high dust-to-ice ratio

(larger than 5), the crystallization front will evolve in a continuous and smooth manner, even if the net energy released is that of pure, amorphous ice. On the other hand, it must be noted that the energy threshold for discontinuous evolution of the crystallization front is close to the lower limit estimated for the energy released during the crystallization of pure, amorphous water ice, 5×10^4 J kg^{-1}, as reported by Hallbrucker & Mayer (1987, See Sect. 2). If this value is representative of the crystallization of cometary, amorphous ice, then the crystallization would probably evolve in a smooth and continuous way, even if it is unaffected by impurities.

4.2. Crystallization-related outbursts?

It is worth discussing the repetitive (or quasi-periodic) spurts of crystallization that occur when the net energy released during crystallization is equal to that of pure, amorphous ice, or is slightly smaller. In principle, these crystallization surges, accompanied of a significant increase in the local temperature, could produce an increase in the pressure of the gas liberated (both because the presence of a spurt implies the rapid liberation of gas and because the local temperature is high). In a future study, we will investigate whether crystallization surges could cause the fracture of material forming the nucleus, by comparing the gas pressures that correspond to the peaks indicated above, with the plausible tensile strength of the cometary material. In any case, these strong increases in the rate of crystallization could produce outbursts. These outbursts would be different from those generally described in the literature (see e.g. Gronkowsky 2007), which appear when the heat wave penetrates deep into the nucleus, raising its interior temperature, and therefore re-activating the crystallization. These normal, and large outbursts, even repetitive, have a timescale that is comparable to the orbital period (Gronkowsky 2007). The possible outbursts observed in the present study would appear once the crystallization started; they have a much higher cadence, and have a far shorter timescale than those previously mentioned. To our knowledge, these rapid and repetitive increases in the crystallization rate have not been previously reported in the cometary literature. Since the model used in this study is very simplified, it would be difficult, and speculative, to extrapolate these results to the possible behavior of comets. Nevertheless, the increases in the crystallization rate described here could be the reason behind the mini outbursts observed in comet Tempel 1, during the intensive campaign of 2005. As reported by A'Hearn et al. (2005), this comet showed 6 mini outbursts in 7 weeks, which were each short in duration. For plausible, physical conditions (density of 400, dust-to-ice ratio of 1, thermal inertia of 20 W K^{-1} m^{-2} s$^{1/2}$), the simulations performed in our study suggest rapid and repetitive increases in the crystallization rate, with a period of approximately 1 week, if the internal temperature is 70 K, and approximately 2 weeks, if the internal temperature is 30 K, a range consistent with the period of the outbursts observed in comet Tempel 1 (1 outburst every 8 days). If the reported outbursts have their origin in the crystallization, then the simulations performed would indicate, on the one hand, that the role of dopant elements, from an energetic standpoint in the crystallization, is comparatively small. On the other hand, the simulations would suggest that, in that case, either the nucleus has a small thermal inertia (~20 W K^{-1} m^{-2} s$^{1/2}$) , a small dust-to-ice ratio (smaller than 1), and a comparatively large internal temperature (70 K), or the nucleus has a moderate-high thermal inertia (100 W K^{-1} m^{-2} s$^{1/2}$), an ice-rich interior (with a dust-to-ice ratio of the order of 0.1), and a cold interior (30 K).

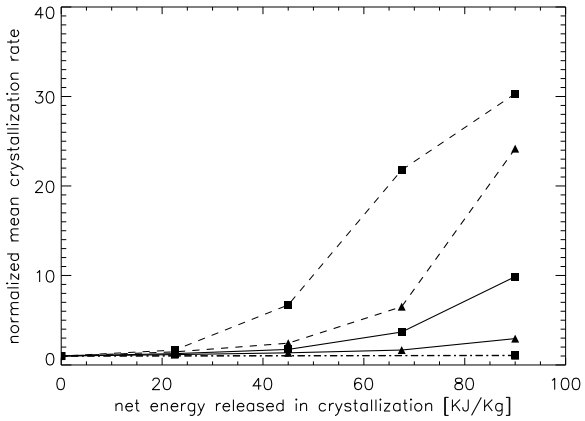

Fig. 3. Normalized mean rate of crystallization for different simulated nuclei as a function of the net energy released during crystallization. All values are normalized to the minimum to show the general tendency. Solid line corresponds to a nucleus with a density of 400 kg m^{-3}, a dust-to-ice ratio of 1, and a thermal inertia of 20 W K^{-1} m^{-2} s$^{1/2}$ (triangles, ▲, when the initial temperature is 30 K and filled squares, ■, when the initial temperature is 70 K). Dashed line represents a nucleus with a density of 400 kg m^{-3}, a thermal inertia of 20 W K^{-1} m^{-2} s$^{1/2}$, and a dust-to-ice ratio of 0.1. As previously, triangles, ▲, when the initial temperature is 30 K and filled squares, ■, when the initial temperature is 70 K. This case shows the largest variation of the mean crystallization rate (for a surface temperature of 160 K) when the net energy released changes. Finally, the dotted-dashed line, which is nearly flat, corresponds to a nucleus with a density of 400 kg m^{-3}, a thermal inertia of 20 W K^{-1} m^{-2} s$^{1/2}$, a dust-to-ice ratio of 20. In this case,simulations with initial temperatures of 30 K and 70 K superimpose.

4.3. Mean rate of crystallization

Figure 3 illustrates the dependence of the mean rate of crystallization on the net energy released during crystallization. The mean crystallization rate was calculated by estimating the time spent in the complete crystallization of the volume from 0.5 m up to 1.5 m. The initial, control point is selected well below the surface to avoid any possible "edge" effect due to the initial, temperature profile. We verified that the mean crystallization rate, estimated from the first half meter of the selected volume, is practically the same as that estimated from the second half meter of the control volume. All curves obtained in the simulations show a similar behavior or dependence. In general, the mean velocity depends exponentially on the net energy released in crystallization. Nevertheless, it can be noted (considering the upper dashed line) that an upper limit to the mean velocity may exist, which is defined by the ability of the medium to transport energy toward the interior. This circumstance may produce the flattening of the profile when the net energy released is high. In principle, all physical parameters that describe the nucleus affect the dependence of the mean crystallization rate on the net energy released, but all simulations show a profile within those shown in the figure. That is, the impact of the net energy released in the mean crystallization rate may range from a practically null effect, when the dust-to-ice ratio is large, to an increase of a factor 30, for ice-rich nuclei.

The impact of the most important parameters on the mean rate of crystallization can be clearly seen in Fig. 4. This figure, which is separated into three plots corresponding to the different dust-to-ice ratios (representing different ice contents, and therefore different quantities to crystallize), shows the mean crystallization rate when the energy released is that of pure amorphous ice, and when the crystallization is neutral from an energetic standpoint. Results are shown for different thermal inertias (20

and 100 W K^{-1} m^{-2} $s^{1/2}$), and different internal temperatures (30 K and 70 K). In this figure, the represented values are the mean obtained by averaging the results of the simulations with different densities (and therefore porosities), but keeping the remainder of the physical characteristics to similar values (i.e. the same dust-to-ice ratio, thermal inertia, and temperature). Error bars represent the dispersion due to the range of densities simulated. In the following description, all the multiplicative factors given are referred to the mean velocity when the transformation is neutral from an energetic point-of-view. Looking at Fig. 4, it can be seen that, logically, the larger the dust-to-ice ratio, the smaller the effect of the net energy released during crystallization. In our simulations, the largest effect of the net energy released during crystallization is obtained for small dust-to-ice ratios. When the dust-to-ice ratio is 0.1, the mean crystallization rate of a nucleus that releases the energy as commonly assumed in cometary, thermophysical models, is a factor of between 20 and 30 (depending on the initial temperature) larger than that of a nucleus in which all the energy released during crystallization is absorbed by the desorption of dopant elements. If the dust-to-ice ratio is 1, the energy released during crystallization may produce an increase that is smaller than an order of magnitude (with respect to the energetically-neutral simulation). When the nucleus is dominated by dust, the net energy released during crystallization hardly affects the mean velocity of crystallization: this behavior, as previously explained, is due not only to the fact that the ice content (and therefore the total energy released) may diminish as the dust-to-ice ratio increases, but also to the fact that the thermal properties, including heat diffusion, are controlled by the dust. This favors heat diffusion toward the interior, while a nucleus that is composed mainly of amorphous ice (below the crystallization front) practically inhibits heat diffusion toward the interior.

We note that the effect of the net energy released in the mean crystallization rate is practically independent of the thermal inertia (for the range of values tested). We mean that the increase in the mean crystallization rate, when the energy released is that of pure, amorphous ice, as opposed to that of an energetically-neutral transition, is approximately the same, regardless of the thermal inertia of our simulations. Only a slight reduction, which is due to the increase in the heat diffusion toward the interior, with no practical effects on thermophysical modeling, was observed. The internal temperature also has an impact, although it is small. Logically, the colder the nucleus interior, the smaller is the effect of the energy released in crystallization. This is because part of the energy has to be expended, before the temperature can increase, with no practical effect on crystallization. The effect of the internal temperature on the crystallization, when it is purely exothermic, is more evident for a dust-to-ice ratio of 1 (See Fig. 3). Under this circumstance, when the initial internal temperature is low, a pure, exothermic crystallization would only increase the mean crystallization rate by a factor 2, or less, compared with the mean rate of an energetically-neutral crystallization. Nevertheless, for temperatures of 70 K, the net energy released may increase the mean rate of crystallization by a factor of the order of 10. For large dust-to-ice ratios, as mentioned above, the net energy released has no practical effect.

4.4. Comparison with erosion rate

The crystallization rates represented in Fig. 4 can be quantitatively compared to surface erosion rates. So far there are several estimates of cometary erosion rates, both observationally derived, and theoretically calculated. To our knowledge, the largest

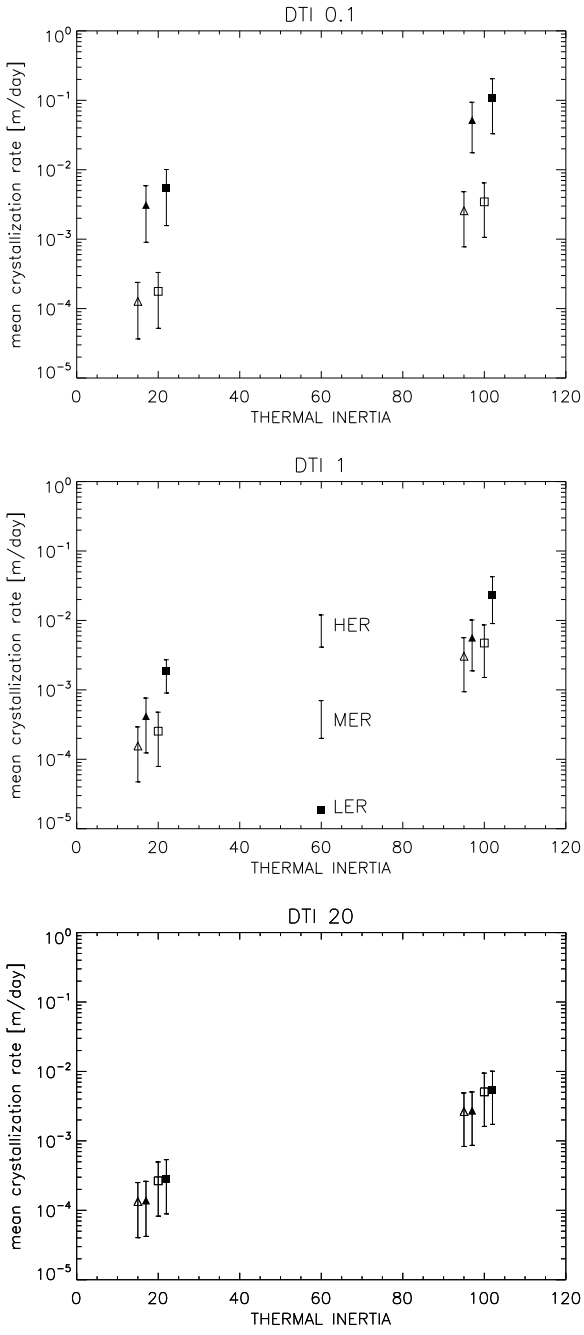

Fig. 4. Mean crystallization rate estimated considering all the simulations both when the net energy released is that of pure amorphous ice (filled symbols) and when the crystallization is energetically neutral (empty symbols). The results are split into three plots, each for a different dust-to-ice ratio. The upper plot corresponds to simulations with a dust-to-ice ratio of 0.1, middle plot to a dust-to-ice ratio of 1, and the lower plot to a dust-to-ice ratio of 20. Inside each plot, symbols on the left correspond to a thermal inertia of 20 W K^{-1} m^{-2} $s^{1/2}$, and those on the right to a thermal inertia of 100 W K^{-1} m^{-2} $s^{1/2}$. Symbols are slightly displaced for clarity. In addition, triangles correspond to simulations where the initial internal temperature is 30 K and squares to simulations with an initial temperature of 70 K. Errors bars represent the dispersion due to the range of densities and porosities simulated (see Table 1). Symbols stand for the mean value. Finally, marks located at a thermal inertia of 60 W K^{-1} m^{-2} $s^{1/2}$ in the middle plot, represent different estimates of the erosion rate, taken from different studies (see text for references). HER, MER, LER represent the ranges of high, medium, and low erosion rates, as found in the literature.

erosion rate ever estimated was that of C/1999 S4 (LINEAR). Both Makinen et al. (2001), and Altenhoff et al. (2004) estimated the erosion rate of this comet, although they obtained very different results. While the former authors obtained an erosion rate of 3.3 m day^{-1}, suggesting that the material of this comet was leaving the nucleus by fragmentation, the latter authors estimated a value of 0.01 m day^{-1}. Given the singularity of comet C/1999 S4 (LINEAR), which fractured, possibly these erosion rates cannot be considered as being regular. Theoretically, Cohen et al. (2003) estimated the erosion rate of a comet in the orbit of comet 46P/Wirtanen. These authors concluded that for a dust-to-ice ratio of 1, and a density of approximately 700 kg m^{-3}, equatorial regions (assuming that the spin axis is normal to the orbital plane) would erode at a rate of 5.7–7 $\times$ 10^{-3} m day^{-1}. Scaling these values to our mean density of 400 kg m^{-3}, the rate would be 7–12 $\times$ 10^{-3} m day^{-1}. Those values are only slightly larger than those obtained by Banaszkiewicz & Rickman (1995) (quoting Rickman 1992). These authors estimated a mean erosion rate of 5.5 $\times$ 10^{-3} m day^{-1}, for a Jupiter-family comet, with a perihelion distance of 1 AU, a period of 6 years, and a density of 300 kg m^{-3}, which is 4.1 $\times$ 10^{-3} m day^{-1} when normalized to a density of 400 kg m^{-3}. The range covered by these estimates is represented in Fig. 4. Henceforth, this set of estimates is referred to as *high erosion rate* (HER). Below that range, Groussin & Lamy (2003) estimated the erosion rate for a nucleus in the orbit of 46P. For a dust-to-ice ratio in the range of 0.5–2, and a density of 1000 kg m^{-3}, these authors calculated that comet 46P would erode at a rate of 2.7 $\times$ 10^{-4} m day^{-1}, that is, 7 $\times$ 10^{-4} m day^{-1} if the density were our mean value of 400 kg m^{-3}. The value obtained by Groussin & Lamy is only slightly larger than the value reported by Keller et al. (2004) for comet Borrelly, 2–4 $\times$ 10^{-4} m day^{-1}, if the bulk density is smaller than 1000 kg m^{-3}. Prialnik (2004) also provides a theoretical expression to estimate the mean erosion per orbit of a comet (see Table 5 in that review). By using that formula, the erosion rate for a typical Jupiter-family comet, with a density of 400 kg m^{-3}, would be approximately 2.3 $\times$ 10^{-4} m day^{-1}, of the same order as the two latter values. The range of values covering the estimates by Groussin & Lamy (2003), Keller et al. (2004), and that of Prialnik et al. (2004) is also represented in Fig. 4. This range can be considered as the *medium erosion rate* (MER). Below that range, we find only the estimate of McDonnell et al. (1987) for comet Halley from Giotto measurements. These authors estimated that the surface of Halley eroded at a rate of 1.8 $\times$ 10^{-5} m day^{-1}. This value, considered as the *low erosion rate* (LER), is also represented in Fig. 4.

We understand that given the uncertainty in the variables involved, and the fact that erosion data are scarce, a direct comparison between crystallization and erosion rates is highly speculative. Nevertheless, thinking of the detection of icy grains in the comae of several comets, presumably in the amorphous state (see Introduction), and given the results obtained in our simulations, it may be worth describing the different possibilities. Considering the simulations performed and assuming always that amorphous ice is (or was) present in cometary nuclei, looking at Fig. 4, it can be seen that if cometary erosion were represented by the *low erosion rate*, it seems that there would not be any possibility to find amorphous ice below the surface. If the erosion rate were that of LER, the crystallization front would evolve faster than the erosion for all ranges of physical parameters tested. At the other end, if the surface eroded at a rate within the *high range*, simulations suggest that amorphous ice could exist comparatively close to the surface, regardless of the energy released during crystallization, if the thermal inertia is very small, of the order of 20 W K^{-1} m^{-2} s$^{1/2}$. If the thermal inertia were of the order of 100 W K^{-1} m^{-2} s$^{1/2}$, simulations suggest that crystallization evolves slower than the HER, except when the dust-to-ice ratio is small (of the order of 0.1) and the energy released is comparatively high (above 45 000 J kg^{-1}). The most complex situation is the comparison between the crystallization rate and a surface eroding at a medium rate (MER). If the erosion rate were MER, the physical circumstances in which crystallization would be slower than the erosion strongly depend on the dust-to-ice ratio. For a dusty nucleus (dust-to-ice ratio of the order of 20), the erosion is faster than the crystallization, regardless of the energy released, provided that the thermal inertia is low (of the order of 20 W K^{-1} m^{-2} s$^{1/2}$). For an icy-nucleus (dust-to-ice ratio of 0.1), in addition to a low thermal inertia, the crystallization must be neutral from an energetic standpoint. A nucleus with a dust-to-ice ratio of 1 would behave similarly to an icy nucleus, except that if the internal temperature is low (of the order of 30 K), even a crystallization releasing the energy of pure, amorphous ice would presumably evolve slower than erosion with MER.

According to the findings obtained from the Deep Impact experiment, the nucleus of Tempel 1 could be a body with a low thermal inertia, and an ice-rich interior. These characteristics could be represented by our simulations with a dust-to-ice ratio of 0.1, and a thermal inertia of 20 W K^{-1} m^{-2} s$^{1/2}$. Under these physical circumstances, if the surface evolved at HER, our simulations suggest that amorphous ice would evolve at a similar rate, and therefore, if it exists, could be located comparatively close to the surface, even for crystallization that released the energy of pure amorphous ice. If the surface evolved at MER, crystallization generally would evolve faster than the surface, except if the energy released during crystallization is smaller than 45 000 J kg^{-1}. Finally, if the surface moved at LER, the crystallization front would evolve faster than the surface regardless of the energy released.

4.5. Effect of surface temperature

The effect of surface temperature is comparatively small compared with the effect of the other parameters described in this section. From our simulations, it is observed that the main effect of increasing the surface temperature is a logical increase in the mean crystallization rate when the net energy released in the transformation is small. This increase is easily explained as due to the augmentation of the energy coming from the boundary. The effect of the surface temperature is less evident when the net energy released is that of pure, amorphous ice. In any case, the net increase in the mean crystallization rate for $H_{\rm net}$ = 0 J kg^{-1}, as the surface temperature increases, translates to a slight variation in the factors given in Fig. 3. We find that the lower the surface temperature, the larger is the difference between the net mean rate when $H_{\rm net}$ is that of pure, amorphous ice compared with that of an energetically-neutral crystallization. From our simulations, the mean crystallization rate, when $H_{\rm net}$ = 0 J kg^{-1}, may increase, at most, by a factor 2 when the temperature increases from 140 K up to 165 K.

5. Summary and conclusions

As seen in the previous section, the net energy released in crystallization may significantly affect both the instantaneous and mean rate of crystallization. The effect of the net energy released depends strongly on the physical properties of the nucleus. Unfortunately, present uncertainty in the basic properties

of cometary nuclei, such as density, thermal inertia, porosity, and dust-to-ice ratio, imply that we cannot determine accurately the effect of the net energy released and that several possible outcomes are equally likely.

Assuming that amorphous ice is (or was) present in cometary nuclei, our simulations imply that

- The effect on thermophysical evolution of the net energy released during crystallization is practically null for a nucleus with a large, dust-to-ice ratio.
- For a nucleus with a dust-to-ice ratio of 1, the net energy released during crystallization may have a strong impact, depending on the internal temperature of the nucleus. If this temperature is approximately 70 K, a pure, amorphous transition will evolve an order of magnitude faster than an energetically-neutral transition. If the nucleus interior were colder, the effect of the net energy released during crystallization would be smaller.
- For an ice-rich nucleus (dust-to-ice ratio of the order of 0.1), the crystallization, when the phase transition is that of pure, amorphous ice, evolves a factor between 20 and 30 times faster than a crystallization neutral from an energetic point-of-view. Findings from the Deep Impact experiment suggest that Tempel-1 could have an ice-rich interior. Therefore, its thermophysical evolution, if this comet had amorphous ice, would depend strongly on the net energy released. Detailed modeling, with a proper treatment of crystallization, is required.
- A proper comparison with erosion rate is not possible because of the large dispersion in its estimates. Nevertheless, simulations suggest that in a large number of physical circumstances it would be possible to find amorphous ice (if it exists) comparatively close to the surface. This implies that the detection of amorphous icy grains is plausible in the coma of some comets, as was the case of C/2002 C7 and Hale-Bopp.

The net energy released during crystallization also significantly affects the instantaneous rate of crystallization. If the dust-to-ice ratio is of the order of (or smaller than) 1, the thermal inertia is comparatively small (smaller than 100 W K^{-1} m^{-2} $s^{1/2}$), and the net energy released is larger than 4.5×10^4 J kg^{-1}, crystallization evolves with quasi-periodic spurts. For other physical circumstances, the crystallization evolves in a continuous and smooth way. The period of the crystallization surges depends strongly on the physical properties of the nucleus, and may range from 1 day up to 1 month (depending on the density, porosity, dust-to-ice, etc.). These crystallization surges could be related to the outbursts observed in Tempel-1 shortly before the Deep Impact experiment.

Finally, it is necessary to point out that given the differences in behavior of our system due to the variation of the net energy released, the porosity, the dust-to-ice ratio, and the conductivity of amorphous water ice, a complete understanding of these phenomena is necessary to develop realistic models of the thermal evolution of doped, amorphous ice in any context, particularly in the astrophysical one. Experiments with large samples of amorphous water ice, co-deposited with other volatile dopants and for various dust-to-ice ratios would be highly desirable. These experiments would allow studies of the evolution of the crystallization front, and the interactions between the gas trapped and the amorphous matrix.

Acknowledgements. The research carried out has been supported by the National Spanish Research Council (CSIC) under project HIELOCRIS (PIF2005) and by the Spanish Ministerio de Educación y Ciencia under project ESP2006-02934. P.J.G. acknowledges financial support from the Spanish Ministerio de Educación y Ciencia (contract "Ramón y Cajal").

References

A'Hearn, M. F., Belton, M. J. S., Crockett, C. J., et al. 2005, BAAS, #37, 1483
Allouche, A., Verlaque, P., & Pourcin, J. 1998, J. Phys. Chem. B, 102, 89
Altenhoff, W. J., Bertoldi, F., Menten, K. M., et al. 2004, A&A, 391, 353
Banaszkiewicz, M., & Rickman, H. 1995, Earth, Moon, and Planets, 71, 203
Bar–Nun, A., & Laufer, D. 2003, Icarus, 161, 157
Bar–Nun, A., Herman, G., Laufer, D., & Rappaport, M. L. 1985, Icarus, 63, 317
Brownlee, D., Tsou, P., Aléon, J., et al. 2006, Science, 314, 1711
Capria, M. T. 2002, Earth, Moon and Planets, 89, 161
Ciesla, F. J. 2007, Science, 318, 613
Cohen, M., Prialnik, D., & Podolak, M. 2003, New A, 8, 179
Colangeli, L., Brucato, B, Bar-Nun, A., Hudson, R. L., & Moore, M. H. 2004, in Comets II, ed. F. Keller, & Weaver (The University of Arizona Press)
Collings, M. P., Dever, J. W., Fraser, H. J., McCoustra, M. R. S., & Williams, D. A. 2003, ApJ, 583, 1058
Davidsson, B. J. R., & Gutiérrez, P. J. 2004, Icarus, 168, 392
Davidsson, B. J. R., & Gutiérrez, P. J. 2005, Icarus, 176, 453
Davidsson, B. J. R., & Gutiérrez, P. J. 2006, Icarus, 180, 224
Davidsson, B. J. R., Gutiérrez, P. J., & Rickman, H. 2007, Icarus, 187, 306
Davies, J. K., Roush, T. L., Cruikshank, D. P., et al. 1997, Icarus, 127, 238
Delsemme, A. H., & Swings, P. 1952, Ann. Astrophys., 15, 1
Ehrenfreud, P., Rodgers, S. D., & Charnley, S. B. 2002, Earth, Moon and Planets, 89, 221
Enzian, A., Cabot, H., & Klinger, J. 1997, A&A, 31, 995
Espinasse, S., Klinger, J., Ritz, C., & Schmitt, B. 1991, Icarus, 92, 350
Flammer, K. R., Mendis, D. A., & Houpis, H. L, G. 1998, ApJ, 494, 822
Gálvez, O., Ortega, I. K., Maté, B., et al. 2007, A&A, 472, 691
Gautier, D., & Hersant, F. 2005, Space Sci. Rev., 116, 25
Groussin, O., & Lamy, P. 2003, A&A, 412, 879
Groussin, O., A'Hearn, M., Li, J.-Y., et al. 2007, Icarus, 187, 16
Ghormley, J. A. 1968, J. Chem. Phys., 48, 503
Gronkowski, P. 2007, Astron. Nachr., 328, 126
Hallbrucker, A., & Mayer, E. 1987, J. Phys. Chem., 91, 503
Herman, G., & Podolak, M. 1985, Icarus, 61, 252
Jenniskens, P., & Blake, D. 1994, Science, 265, 753
Kawakita, H., Watanabe, J., Ootsubo, T., et al. 2004, ApJ, 601, L191
Keller, H. U., Britt, D., Buratti, B. J., et al. 2004, In Comets II, ed. M. Festou, H. U. Keller, & H. A. Weaver (University of Arizona Press)
Klinger, J. 1981, Icarus, 47, 320
Kouchi, A., & Sirono, S. 2001, Geophys. Res. Lett., 28, 827
Küppers, M., Bertini, I., Fornasier, S., et al. 2005, Nature, 437, 987
Lisse, C. M., A'Hearn, M., Groussin, O., et al. 2005, ApJ, 625, 139
Sirono, S., & Yamamoto, T. 1999, Advanced Space Research, 23, 1299
Macfarlane, D. R., & Angell, C. A. J. 1984, Phys. Chem., 88, 759
Makinen, J. T. T., Bertaux, J. L., Combi, M. R., et al. 2001, Science, 292, 1326
Manca, C., Martin, C., Allouche, A., & Roubin, P. 2001, J. Phys. Chem. B, 105, 12861
McDonnell, J. A. M., Zarnecki, J. C., Olearczyk, R. E., et al. 1987, Phil. Trans. R. Soc. Lond. A, 323, 381
Moore, M. H., Ferrante, R. F., Hudson, R. L., et al. 1994, ApJ, 428, L81
Prialnik, D. 1992, ApJ, 388, 196
Prialnik, D., Benkhoff, J., & Podolak, M. 2004, in Comets II, ed. M. Festou, H. U. Keller, & H. A. Weaver (University of Arizona Press)
Rickman, H. 1992, In Interrelations between Physics and Dynamics for Minor Bodies in the Solar System, ed. D. Benest, & C. Froeschlé
Richardson, J. E., & Melosh, H. J. 2006, LPI, 36, 1836
Sandford, S. A., & Allamandola, L. J. 1990, Icarus, 87, 188
Schmitt, B., Espinasse, S., Grim, R. J. A., Greenberg, J. M., & Klinger, J. 1989, Physics and Mechanics of Cometary Material, 65
Sunshine, J. M., Groussin, O., & Schultz, P. H. 2007, Icarus, in press
Tancredi, G., Rickman, H., & Greenberg, J. M. 1994, A&A, 286, 659
Yue, Y., & Angell, C. A. 2004, Nature, 427, 717